ORIGINAL ARTICLE—ALIMENTARY TRACT

Role of miR-19b and its target mRNAs in 5-fluorouracil resistance in colon cancer cells

Ken Kurokawa · Toshihito Tanahashi · Tsutomu Iima · Yuta Yamamoto ·
Yoko Akaike · Kensei Nishida · Kiyoshi Masuda · Yuki Kuwano ·
Yoshiki Murakami · Masakazu Fukushima · Kazuhito Rokutan

Abstract

Background Drug resistance in colorectal cancers is assumed to be mediated by changes in the expression of microRNAs, but the specific identities and roles of microRNAs are largely unclear. We examined the effect of 5-fluorouracil (5-FU) resistance on microRNA expression.
Methods Two types of 5-FU-resistant colon cancer cells were derived from the DLD-1 and KM12C cell lines. The expressions of microRNAs were profiled with a microarray containing 723 microRNAs and validated by quantitative real-time polymerase chain reaction (qRT-PCR). To survey the downstream mediators of microRNA, we used a microRNA:mRNA immunoprecipitation (RIP)-Chip and pathway analysis tool to identify potential direct targets of microRNA.

Results In response to 5-FU, miR-19b and miR-21 were over-expressed in 5-FU-resistant cells. Of note, miR-19b was up-regulated 3.47-fold in the DLD-1 resistant cells, which exhibited no alteration in cell cycle profiles despite exposure to 5-FU. After transfection of miR-19b, specific mRNAs were recruited to microRNA:mRNA complexes isolated with Ago2 antibody and subjected to whole-genome transcriptional analysis. In this analysis, 66 target mRNAs were enriched by at least 5.0-fold in the microRNA:mRNA complexes from DLD-1 resistant cells. Ingenuity pathway analysis of mRNA targets significantly ($P < 0.05$) indicated the category "Cell Cycle" as a probable area of the molecular and cellular function related with 5-FU resistance. Among candidate mRNA targets, *SFPQ* and *MYBL2* have been linked to cell cycle functions.
Conclusions We revealed up-regulation of miR-19b in response to 5-FU and potential targets of miR-19b mediating the cell cycle under treatment with 5-FU. Our study provides an important insight into the mechanism of 5-FU resistance in colorectal cancers.

Keywords Colorectal cancer · 5-Fluorouracil · microRNA · RIP-Chip

K. Kurokawa · T. Tanahashi · T. Iima · Y. Yamamoto ·
Y. Akaike · K. Nishida · K. Masuda · Y. Kuwano · K. Rokutan
Department of Stress Science, Institute of Health Biosciences,
The University of Tokushima Graduate School,
Tokushima 770-8503, Japan

T. Tanahashi (✉)
Division of Gastroenterology, Department of Internal Medicine,
Kobe University Graduate School of Medicine,
7-5-1 Kusunoki-cho, Chuo-ku, Kobe 650-0017, Japan
e-mail: tana@med.kobe-u.ac.jp

Y. Murakami
Center for Genomic Medicine, Kyoto University Graduate
School of Medicine, Kyoto 606-8507, Japan

M. Fukushima
Personalized Medication Research Laboratory, Taiho
Pharmaceutical Company, Ebisuno, Tokushima 771-0194, Japan

Introduction

Colorectal cancer is the leading cause of cancer-related deaths in Western countries [1]. The anti-metabolite 5-fluorouracil (5-FU) is one of the most active drugs against this malignancy [2]. Recently, efforts to improve the efficacy of 5-FU have led to new combination therapies with other anticancer drugs, and these therapies have significantly improved the response rates, to 40-50%, and prolonged overall survival [3]. However, there remain

several problems associated with effective cancer treatment. Above all, cancer cells can acquire resistance to chemotherapy through complex mechanisms, including DNA mutation, over-expression of the drug target, and inactivation or elimination of the drug [4].

Several studies have attempted to define the molecular and biochemical mechanisms of responses to chemotherapy. Of note, the introduction of microarray technology has revolutionized the approach to understanding the molecular events regulating the drug-resistant phenotype, allowing the simultaneous assessment of more than tens of thousands of genes [5]. However, to date, no convincing finding has been observed in simple gene expression profiles to predict the response to 5-FU [6–9]. This implies that multiple, distinct factors may determine inherent and acquired 5-FU resistance.

Small non-coding RNAs in the size of 19–25 nucleotides (nt), called microRNAs, are cleaved from 70- to 100-nt hairpin pre-microRNA precursors [10, 11]. Mature microRNAs are genetically conserved sequences that play important roles in the control of gene expression by blocking the translation of mRNA into protein and/or by promoting the degradation of several target mRNAs [12, 13]. The number of known microRNAs has rapidly increased, and there are now over 900 human microRNA sequences deposited in the Sanger Institute's miRBase, with potentially many more to be reported [14]. Recent intensive studies have revealed that microRNAs are involved in numerous biological processes, including cell proliferation, differentiation, and cell death [15]. In addition, microRNAs have been shown to be aberrantly expressed in certain tumors and to serve as oncogenes or tumor suppressive genes [16]. Thus, microRNAs have been implicated in the regulation or modulation of cell cycle control in various types of tumors [17].

Given these features of microRNAs, the mechanisms of anticancer drugs could partly rely on their influence on microRNA expression. For example, the expression of miR-21 was found to confer insensitivity to topotecan (a clinical camptothecin analogue) in tumor cells, in addition to promoting cell proliferation and growth [18]. More recently, the up-regulation of miR-214 promoted the survival of ovarian cancer cells and induced resistance to cisplatin [19]. Based upon these novel pharmacological insights, microRNAs could be involved in numerous other drug responses in cancer cells.

In this study, we examined the effect of the widely used anticancer drug 5-FU on microRNA expression profiles in colon cancer cells. We identified the up-regulation of specific microRNA expression in response to 5-FU treatment. To further determine which genes were responsible for the control of microRNA, the microRNA:mRNA immunoprecipitation (RIP)-Chip method was applied to identify the predicted target genes of microRNA.

Materials and methods

The detailed study protocol is described in the supplementary material.

Reagents, cell lines, and cell cultures

5-Fluorouracil (5-FU) was purchased from Sigma-Aldrich (St. Louis, MO, USA). The human colon cancer cell lines DLD-1 and KM12C and their drug-resistant counterparts, DLD-1/R and KM12C/R, were provided by Taiho Pharmaceutical (Tokushima, Japan).

DLD-1/R cells were originally derived from the DLD-1 cell line by continuous in vitro exposure to increasing concentrations of 5-FU through a number of successive passages, as described earlier [20]. KM12C/R cells were established by in vivo passaging to implant into nude mice [21]. DLD-1 and its resistant line were cultured in RPMI 1640 medium (Sigma) containing 10% fetal bovine serum (FBS) and 1% penicillin–streptomycin. KM12C cells were grown in Eagle's MEM (Sigma) with 10% FBS.

Cell proliferation assay

Cell growth was assayed using the CellTiter 96 AQueous One Solution Cell Proliferation Assay (Promega, Madison, WI, USA). Cell growth was assayed in 96-well plates after 0, 6, 12, 24, 48, and 72 h without 5-FU treatment. Cells were also treated with various concentrations of 5-FU, of up to 60 μM. MTT reagent (20 μl/well) was added, and the plates were incubated at 37°C for 1 h. The levels of blue formazan were measured spectrophotometrically at 490 nm using a micro-plate reader (Wallac 1420 ARVO MX; Perkin-Elmer, Boston, MA, USA). Results are expressed as the mean absolute absorbance divided by the mean absolute absorbance of the control sample. Results of >1.0 indicate proliferation, whereas results of <1.0 indicate growth inhibition.

Flow cytometry cell cycle analysis

Cell cycles were analyzed by flow cytometry as previously described [22]. Cells were treated with a range of 5-FU concentrations (0, 1, 10, 20, 30, and 60 μM). After 72-h treatment, the cells were washed, fixed with 70% ethanol, and incubated for 30 min at 37°C with 1 mg/ml RNase in phosphate-buffered saline (PBS). The cells were stained in PBS containing 100 μg/ml propidium iodide (PI) for 30 min at room temperature. The cell count was analyzed

with a Beckman Coulter Epics XL flow cytometer (Miami, FL, USA). Data were analyzed using FlowJo (Tree Star, Ashland, OR, USA).

RNA isolation

Cells were treated with 60 μM of 5-FU for 72 h, and this was the same condition as that used for the analysis of the cell cycle. RNAs were collected before (0 h) and after the treatment with 5-FU (72 h). A total of 8 RNAs were sampled for the analysis, as outlined in Fig. S1.

An miRNeasy mini kit (Qiagen, Valencia, CA, USA) was used to extract total RNA including microRNA. The RNA quantity and quality were measured with an ND-1000 spectrophotometer (Nanodrop, Wilmington, DE, USA) and a 2100 Bioanalyzer (Agilent Technologies, Palo Alto, CA, USA), respectively. High-quality RNA (i.e., RNA integrity number >8.5) was used for experiments [23]. Three independent RNA samples were pooled, to reduce the biological variability, as previously recommended [24]. Each RNA sample was then split into two aliquots that were processed for either microarray or quantitative real-time polymerase chain reaction (qRT-PCR).

microRNA microarray and data analysis

Expressions of microRNA were explored using an Agilent human microRNA microarray (G4471A). This microarray consists of 60-mer DNA probes, which represent 723 human and 76 human viral microRNAs from the Sanger miRBase release 10.1. One-color microRNA labeling with Cy3 fluorescence, hybridization, and washing were performed in accordance with the manufacturer's instructions. The array was scanned with a laser scanner (G2565BA; Agilent) and Feature Extraction 9.5 (Agilent) was used to obtain raw data.

Data were analyzed using GeneSpring GX10.0.2 (Agilent). Quality control (QC) was applied according to the manufacturer's instructions, and all data were approved. Following Agilent recommendations, no inter-array normalization was applied because the similarity of microRNA expression among sample arrays was unknown [25]. Filtering by "Flag at Present" in at least one sample was applied. We further selected probes having fluorescence intensities of >100 from at least one sample among 8 samples. Differentially expressed microRNAs were identified with a filter based on a fold change of 2.0. Principal component analysis (PCA) was performed with Gene-Spring. Hierarchical clustering was also generated using an unsupervised method. Pearson's correlation coefficients were calculated between technical replicates to assess variations introduced by microRNA extraction, labeling, and hybridization, and slide heterogeneity. The complete

datasets were deposited in the Gene Expression Omnibus database (accession number GSE30894).

Quantitative real-time PCR (qRT-PCR) of microRNA

RNA samples were prepared using the same protocol as that used for the microarray analysis. Quantitative stem-loop reverse transcription was performed with a TaqMan microRNA RT kit (Applied Biosystems, Foster City, CA, USA). The PCR primers and probes for hsa-miR-19b (AB assay ID; 000396) and hsa-miR-21 (ID; 000397) were purchased from the manufacturer. For RT reactions, 10 ng total RNA was used in each reaction and mixed with the RT primer.

The relative expression levels of microRNAs were calculated from a standard curve. qRT-PCR reactions were run on an ABI Prism 7900HT (Applied Biosystems) and analyzed using SDS software (Applied Biosystems). Pearson's correlation coefficients were calculated from the values between the microarray raw signal and the cycle threshold (Ct) value of qRT-PCR.

Transfection of microRNAs

The pre-miR-19b precursor (PM10629) and a control precursor (scramble) were purchased from Ambion (Austin, TX, USA). Pre-miR-19b (15 nM) and the scrambled control (30 nM) were transfected into DLD-1 and DLD-1/R cells grown at 1×10^6 cells/dish in 10-cm dishes 24 h before transfection. Transfection was done with RNAi-MAX (Invitrogen, Carlsbad, CA, USA).

microRNA:mRNA immunoprecipitation (RIP)-Chip with anti-Ago2

microRNA:mRNA immunoprecipitation was performed using the Magna RIP kit (Millipore, Billerica, MA, USA) following the manufacturer's protocol. Cells were scraped off 24 h after transfection with either the pre-miR-19b or the scrambled sequence. Cells were then lysed in complete RIP lysis buffer, after which 100 μl of whole cell extract was incubated with RIP buffer containing magnetic beads conjugated with human anti-Ago2 antibody (Millipore) or negative control normal mouse IgG (Millipore) and rotated for 3 h at 4°C. Samples (20 μl) were analyzed by western blotting, using anti-Ago2 antibody (1:1000) (Wako Chemical, Osaka, Japan) to check immunoprecipitation (IP) efficiency. The remaining samples were incubated with Proteinase K with shaking to digest the protein. Co-immunoprecipitated RNA, including microRNA:mRNA complexes, was subjected to microarray analysis.

A low RNA Fluorescent Linear Amplification Kit PLUS One Color (Agilent) was used to make cRNA from

co-immunoprecipitated RNA. The synthesized cRNA was labeled with Cy3. cRNA was applied to human whole genome microarray (4 × 44 k; Agilent). Signal intensities were quantified with the Feature Extraction 9.5 (Agilent). The signal intensities from the Ago2-IP and mouse IgG-IP were compared between miR-19b and the control (scramble) transfected samples. Gene transcripts corresponding to an Ago2-IP/IgG-IP ratio of >5.0-fold were considered to indicate enrichment in the Ago2-IP fraction [26].

Target prediction of microRNA and functional analysis of identified mRNAs

TargetScan Human release 5.2 (http://www.targetscan.org/) was used to predict the target of miR-19b. Using Target-Scan, 2616 targets were predicted irrespective of site conservation. We also used Ingenuity Pathway Analysis (IPA) 9.0 (http://www.ingenuity.com/) to determine functional pathways for the mRNAs identified in the Ago2-IP fraction [27]. IPA incorporates most of the knowledge in the literature about biological interactions among genes and proteins, and we used it to calculate the probability of a relationship between each pathway and the identified genes.

Results

Cell proliferation

Figure 1a shows the time-response curves for DLD-1 and DLD-1/R cells without 5-FU treatment. There was no remarkable difference between the parental and resistant cells until 72 h. Similarly, KM12C parental and resistant cells showed no difference in cell growth through 72 h (Fig. 1b). The cytotoxic effects of DLD-1 parental cells were consistent with the inhibitory concentration (IC_{50}) described in a previous report (5.87 μM) [20]. In contrast, we found no cytotoxic effect of 5-FU against DLD-1/R cells until the 60-μM concentration (Fig. 1c). However, subtle cytotoxic effects were observed in KM12C/R, although these cells showed a 2.0-fold greater tolerance than sensitive cells up to the 60-μM concentration (Fig. 1d).

Cell cycle analysis after 5-FU treatment

Flow cytometry was used to examine cell cycle distribution after treatment with a range of concentrations of 5-FU (Fig. 1e, f). Percentages of cells at each cycle phase are shown in Table S1. After exposure to increasing concentrations of 5-FU from 10 to 60 μM, the majority of DLD-1 cells moved to S and G_2–M phase, and the proportion of G_1

cells decreased to a level comparable to that of untreated cells (Fig. 1e). However, DLD-1/R cells showed no change in cell cycle profile after the exposure to 5-FU; the proportion of cells arrested at the G_1 phase was in the range of 65.2–70.9% (67.5% in no-treatment cells) (Fig. 1e). In contrast, the cell cycle distribution of KM12C/R cells changed with increasing concentrations of 5-FU, from 10 to 60 μM of 5-FU. These cells moved to S and G_2–M phases, and there was a decreased proportion of G_1 phase compared with that in untreated cells. These cell cycle profiles indicate differences between cell lines that may underlie resistant phenotypes.

Identification of specific microRNA expression after 5-FU treatment

To identify microRNAs differentially expressed in response to 5-FU, we collected 8 RNA samples from cells and compared their expression profiles. The results of duplicate arrays using the same RNA source were highly correlated (Pearson's correlation coefficients; 0.999–0.993) (Fig. S2). All microarray data passed the QC recommended by the manufacturer.

Of the 723 microRNAs, 5 microRNAs not present in release 12.0 (September 2008) were excluded, and the remaining 718 microRNAs were used for further analysis. These probes were also subjected to PCA, and 8 principal components were identified based on their etiology (Fig. 2a).

Of the 718 probes, 223 probes were passed over the threshold of "Flag at Present". Followed by further filtering for raw signal intensity of >100 in at least one sample, 56 human miRNAs remained. As shown in Fig. 2b, unsupervised hierarchical clustering using 56 microRNAs generated a tree with a branch representing their cellular etiology.

Using the criterion of expression change of >2.0-fold after treatment with 5-FU, we surveyed differentially expressed microRNAs. Venn diagrams showed that some types of microRNAs were differentially regulated in 5-FU-sensitive and -resistant cells (Fig. 2c). In DLD-1 parental and resistant cells, a total of 47 microRNAs were differentially expressed by >2.0-fold after exposure to 5-FU. Eight microRNAs were specifically up-regulated in DLD-1/R cells (Table 1), whereas a total of 33 microRNAs were up-regulated in KM12C and KM12C/R cells, and 22 microRNAs were specifically up-regulated in KM12C/R cells (Table 1). We found up-regulation of miR-130b expression in both DLD-1/R and KM12C/R cells, but their expression levels were relatively low against the thresholds. There were no down-regulated microRNAs after the 5-FU treatment. These results suggested the possibility that specific microRNAs are expressed in specific drug-resistant cells.
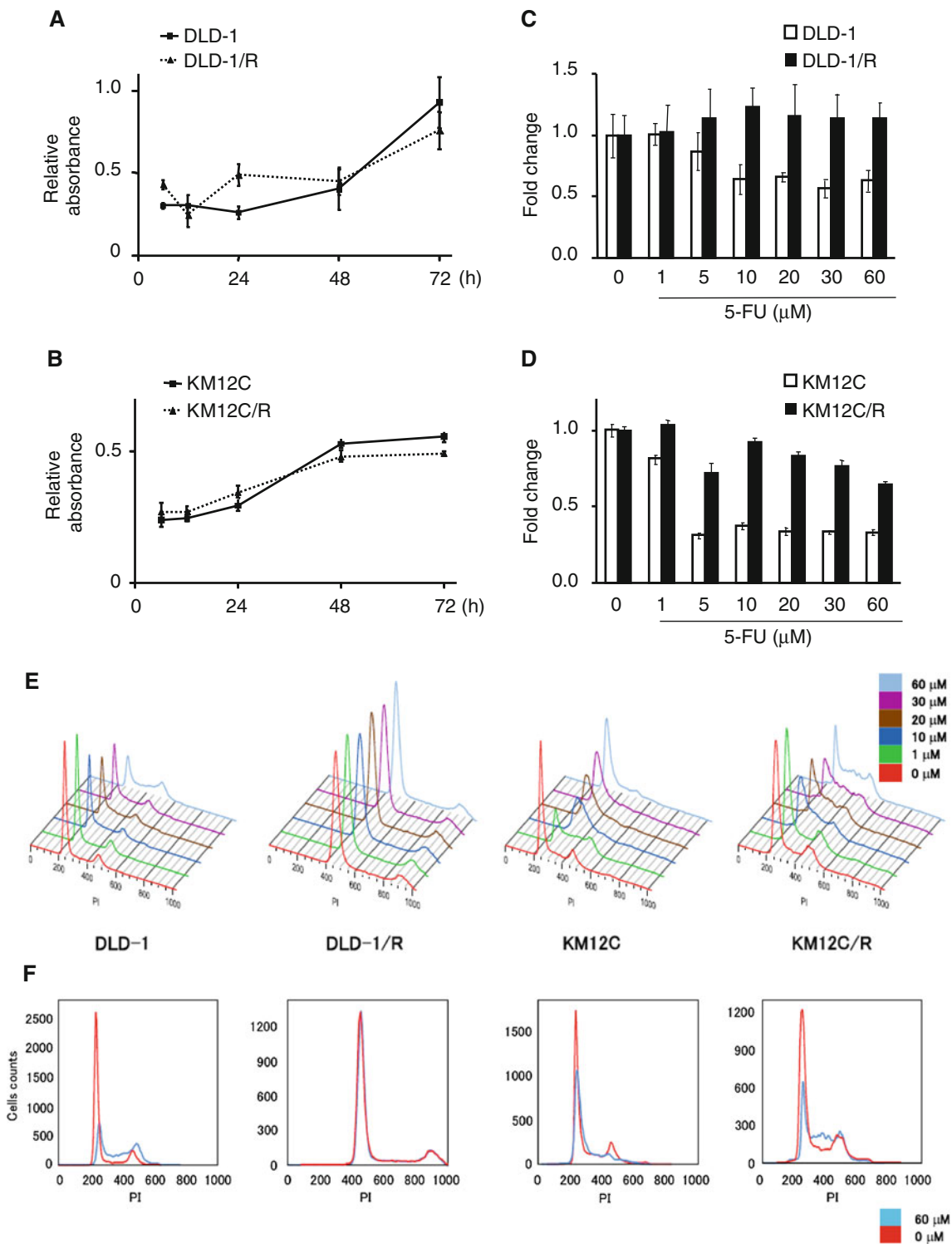
Fig. 1 5-Fluorouracil (*5-FU*) suppresses the proliferation of DLD-1 and KM12C cells (drug-sensitive), but not DLD-1/R and KM12C/R cells (drug-resistant). **a, b** Proliferation assays for 5-FU-sensitive and -resistant cells. Viable cells were counted, using MTT assays, at 6, 12, 24, 48, and 72 h. Results are presented as the means ± SD of absolute absorbance in triplicate. **c, d** Cytotoxicity assays for 5-FU-sensitive and -resistant cells. 5-FU induced no cytotoxicity against DLD-1/R cells until a 60-μM concentration of 5-FU. All measurements were done in triplicate. *Bars* indicate SD values in triplicate experiments. **e** Cell cycle of 5-FU-sensitive and -resistant cells following 5-FU treatment at 72 h. Data are presented as histogram overlay scaling options, in which the area under each curve corresponds to all gated cells. **f** Data are presented as normal histograms. Fluorescent intensities of propidium iodide (*PI*) are indicated on the *x* axis, and the cell count is shown on the *y* axis. The precise percentage of cell cycle phases is shown in Table S1
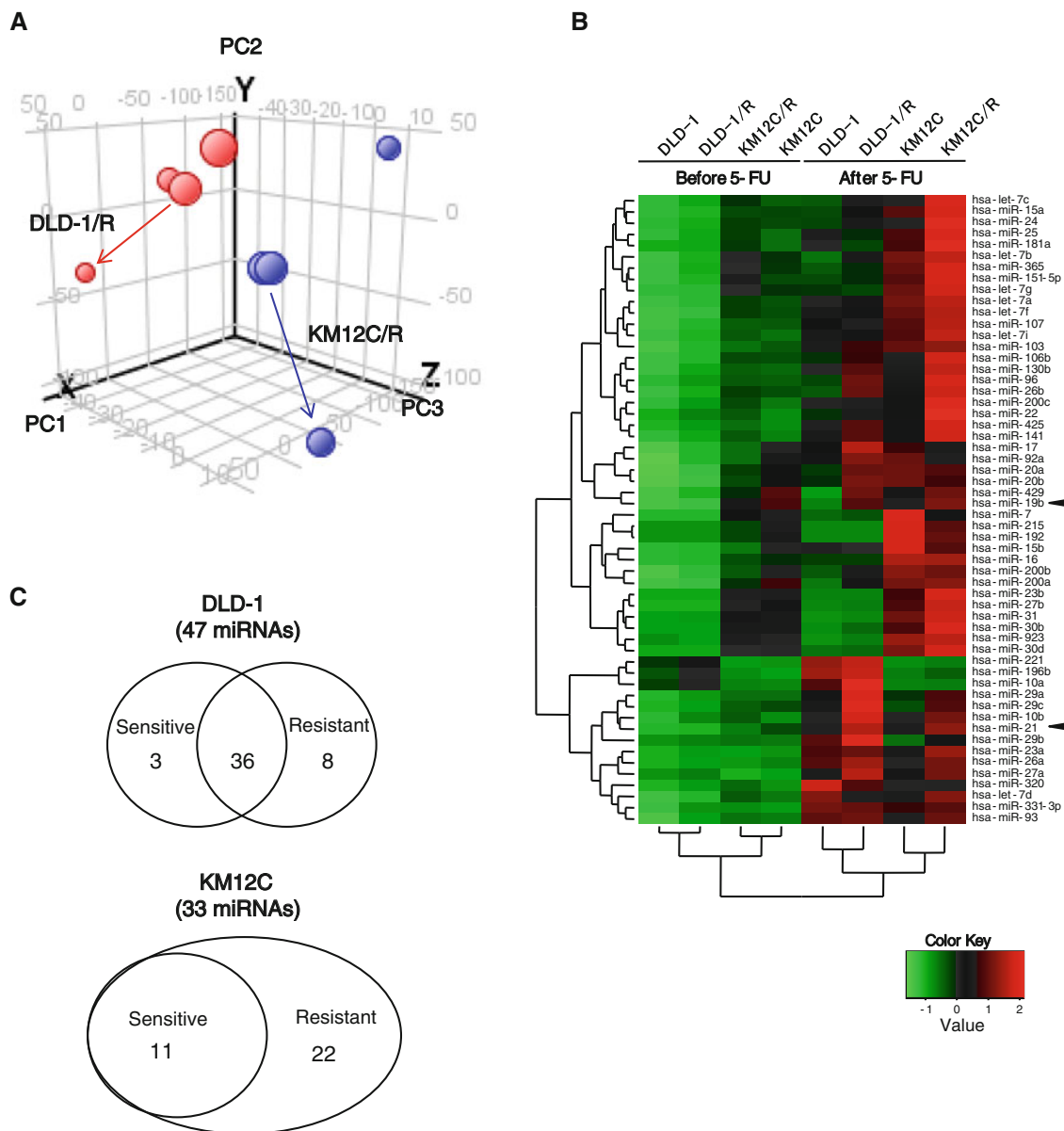
Fig. 2 Principal component analysis (PCA), unsupervised hierarchical clustering, and Venn diagrams between differentially expressed microRNAs. **a** Shown here are 8 principal components of the expression profile of 718 microRNAs. DLD-1 and DLD-1/R cells are depicted as *blue*. KM12C series are in *red*. Without treatment with 5-FU, the principal components from sensitive and resistant cells formed clusters according to their origins. After the exposure to 5-FU, these clusters separated and became distinct from one another. *PC1 PC2* **b** Unsupervised hierarchical clustering generated 56 microR-NAs. *Each column* represents one microRNA, and *each row* represents their cellular origin. A pseudo-colored representation of the relative intensity is shown, such that a *red color* indicates high expression and *green color* low expression. Before exposure to 5-FU, microRNA expression was low in both DLD-1 and KM12C cells. After treatment, microRNA expression was especially high in the resistant cells. *Black arrows* indicate the position of miR-19b and miR-21. **c** Venn diagrams illustrate the relationship between the sets of differentially expressed microRNAs. microRNAs were differentially expressed among DLD-1 and KM12C cells, and their resistant cells. The number of microRNAs shared between each comparison is indicated in the *overlapping area*

Confirmation of miR-19b and miR-21 expressions by qRT-PCR

On the basis of previously reported biological functions [18, 28–30], we selected two microRNAs, miR-19b and miR-21, and assayed them to validate our microarray data.

We used the same RNA samples as those used in the microarray analyses. All measurements were done in triplicate. The mean expression values of each experiment are shown in Fig. 3. The values obtained from the microarray and qRT-PCR analyses were highly correlated (Pearson's correlation coefficients 0.911 for miR-19b and 0.932 for

Table 1 List of microRNAs differentially expressed in response to 5-fluorouracil (FU) in resistant cells

miRNA	DLD-1/R		Fold change	DLD-1		Fold change	Accession number
	0 h	72 h		0 h	72 h		
(A) 8 miRNAs up-regulated in DLD-1/R cells							
let-7b	199.5	404.0	2.02	154.5	277.3	1.79	MIMAT0000063
let-7c	76.3	159.6	2.09	64.1	107.8	1.68	MIMAT0000064
miR-130b	43.5	120.9	2.78	NA	NA	NA	MIMAT0000691
miR-19b	**78.2**	**271.9**	**3.47**	**67.9**	**130.8**	**1.92**	**MIMAT0000074**
miR-20b	44.9	149.4	3.32	NA	NA	NA	MIMAT0001413
miR-29c	43.5	160.9	3.70	NA	NA	NA	MIMAT0000681
miR-429	33.5	113.7	3.39	NA	NA	NA	MIMAT0001536
miR-96	35.9	122.7	3.41	NA	NA	NA	MIMAT0000095
miRNA	KM12C/R		Fold change	KM12C		Fold change	Accession number
	0 h	72 h		0 h	72 h		
(B) 22 miRNAs up-regulated in KM12C/R cells							
let-7e	62.4	153.5	2.45	NA	NA	NA	MIMAT0000066
let-7g	359.1	775.8	2.16	341.0	606.8	1.77	MIMAT0000414
miR-103	190.2	391.7	2.05	207.3	359.7	1.73	MIMAT0000101
miR-106b	153.6	376.2	2.44	150.2	246.6	1.64	MIMAT0000680
miR-107	363.1	826.9	2.27	368.8	659.0	1.78	MIMAT0000104
miR-130b	65.0	151.3	2.32	61.2	105.3	1.72	MIMAT0000691
miR-141	114.0	291.4	2.55	90.6	172.5	1.90	MIMAT0000432
miR-15a	147.9	397.8	2.68	150.4	286.8	1.90	MIMAT0000068
miR-15b	360.3	813.3	2.25	559.2	1113.1	1.99	MIMAT0000417
miR-181a	52.2	162.2	3.10	NA	NA	NA	MIMAT0000256
miR-200c	895.6	2214.6	2.47	697.3	1209.5	1.73	MIMAT0000617
miR-21	**2829.8**	**7196.6**	**2.54**	**3717.4**	**4618.0**	**1.24**	**MIMAT0000076**
miR-24	288.5	710.8	2.46	273.9	438.6	1.60	MIMAT0000080
miR-25	152.1	335.7	2.20	123.1	239.5	1.94	MIMAT0000081
miR-26a	49.6	133.9	2.70	NA	NA	NA	MIMAT0000082
miR-26b	125.4	284.6	2.27	116.8	167.4	1.43	MIMAT0000083
miR-30b	76.3	188.0	2.46	76.8	116.1	1.51	MIMAT0000420
miR-30d	106.6	284.1	2.66	111.5	218.2	1.95	MIMAT0000245
miR-31	157.1	324.3	2.06	134.1	243.1	1.81	MIMAT0000089
miR-365	51.7	111.5	2.15	NA	NA	NA	MIMAT0000710
miR-425	36.4	114.8	3.15	NA	NA	NA	MIMAT0003393
miR-96	56.9	158.5	2.78	NA	NA	NA	MIMAT0000095

Boldface items indicate microRNAs used for validation by quantitative real-time polymerase chain reaction (qRT-PCR) in this study. *NA* denotes "Flag at Absent"

miR-21). The microarray result indicates a consistent with the qRT-PCR data, as supported by a recent report [31].

miR-19b transfection and RIP-Chip assay

The design of the RIP-Chip assay is shown in Fig. 4a. Following transfection, we identified miR-19b as a microRNA up-regulated in DLD-1/R cells, and which showed no alteration in cell cycle profile after exposure to 5-FU.

The effectiveness and specificity of miR-19b transfection was evaluated with qRT-PCR (Fig. 4b). RNAs were isolated from DLD-1 and DLD-1/R cells 24 h after the transfection of the pre-miR-19b precursor. Transfected pre-miR-19b was appropriately incorporated into cells as mature miR-19b, as validated by qRT-PCR.

To test whether miR-19b had an effect on the target gene, we next analyzed Ago2-associated mRNAs by microarray analysis. Microarray results were obtained

Fig. 3 Comparison of quantitative real-time polymerase chain reaction (*qRT-PCR*) and microarray expression profiles. **a** miR-19b in DLD-1 and its resistant cells. **b** miR-21 in KM12C and its resistant cells. In the correlation plots (*left*), raw signal data from microarrays are indicated on the *y* axis as $\log_2$ scale, and the cycle threshold (*Ct*) values with qRT-PCR are indicated on the *x* axis. Triplicate assays were performed for each RNA sample, and the mean expression values of each experiment are shown. High correlations were observed (Pearson's correlation coefficients 0.911 for miR-19b and 0.932 for miR-21). In the bar plots (*right*), results are plotted for each microRNA with microarray (*white*) and qRT-PCR (*black*). Error bars indicate one standard deviation. *S* sensitive, *R* resistant
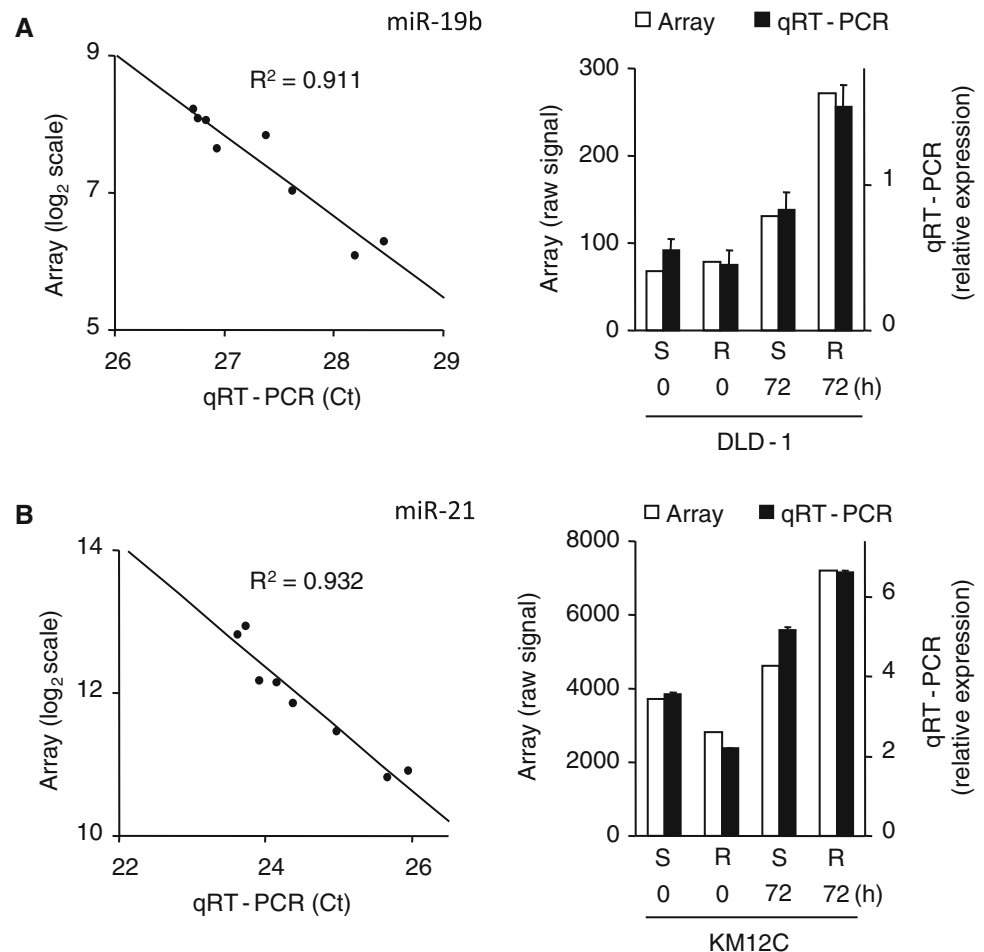
from DLD-1 and DLD-1/R cells transfected with pre-miR-19b and a control (scrambled) sequence. Anti-Ago2 antibody [26, 32, 33] was used to pull down endogenous Ago2-containing microRNA:mRNA complexes. Western blotting of co-immunoprecipitates showed that Ago2 was specifically isolated with the anti-Ago2 antibody, but not with mouse IgG, in both DLD-1 and DLD-1/R cells (Fig. 4c).

Figure 4d shows the results of mRNA microarray analysis as relative enrichment of target mRNAs. We defined target mRNAs as enrichment of signal intensities of >5.0-fold in the Ago2-IP/IgG-IP fraction. Following transfection of miR-19b, RIP-Chip revealed a relative enrichment of 128 mRNAs in the Ago2-IP/IgG-IP fraction. In DLD-1 cells, 62 target mRNAs were detected, and all 62 mRNAs showed no enrichment with transfection by a control sequence. In DLD-1/R cells, 66 target mRNAs were shown to be enriched in the IP fraction after transfection by miR-19b. Of note, there were no common mRNAs enriched in the Ago2-IP fractions of both DLD-1

and DLD-1/R cells. Table 2 indicates the 15 target mRNAs most enriched in the Ago2-IP/IgG-IP fraction.

Target prediction of microRNAs and functional analysis of RIP-Chip data

We compared the RIP-Chip data using the computational target prediction program "TargetScan". Not all gene transcripts were included in the database for prediction (Table 2). IPA was used to organize the target mRNAs of miR-19b into functionally annotated pathways. In the top 5 bio functions of molecular and cellular functions, the category "Cell Cycle" was significantly ($P < 0.05$) indicated both in DLD-1 and DLD-1/R cells (Table 3). In DLD-1 cells, 10 molecules were listed in the category "Cell Cycle"; *GRK4*, *RBBP8*, *IFNB1*, *RAC1*, *RPS6*, *FGFR2*, *SCMH1*, *KAT2A*, *PSEN1*, and *ARID3A*. In contrast, only *SFPQ* and *MYBL2* were included in the category "Cell Cycle" for DLD-1/R cells. After the transfection of miR-19b, *SFPQ* and *MYBL2* mRNAs were certainly included in

Fig. 4 Identification of Ago2-associated microRNA:mRNA complexes and target mRNAs with RIP-Chip. **a** Schematic illustration of the RIP-Chip method–microRNA:mRNA complexes were co-immunoprecipitated with anti-Ago2 antibody bound to magnetic beads. mRNAs associated with Ago2 protein were processed for human whole genome microarray. **b** qRT-PCR shows that the expression of miR-19b was increased to about 800-fold that expected after the transfection of the pre-miR-19b precursor, but not control precursor. **c** Co-immunoprecipitation (*IP*) and input products (1/4 of cell lysates) analyzed by western blotting (*WB*) with anti-Ago2 antibody. Co-IPs were performed on cells transfected with pre-miR-19b precursor. As expected, Ago2 proteins were co-immunoprecipitated with anti-Ago2, but not with mouse IgG in DLD-1 and DLD-1/R cells. **d** Venn diagrams illustrate the number of target mRNAs with RIP-Chip analysis. **e** Ago2-associated microRNA:mRNA complexes contain *SFPQ* and *MYBL2* mRNAs after transfection of the pre-miR-19b
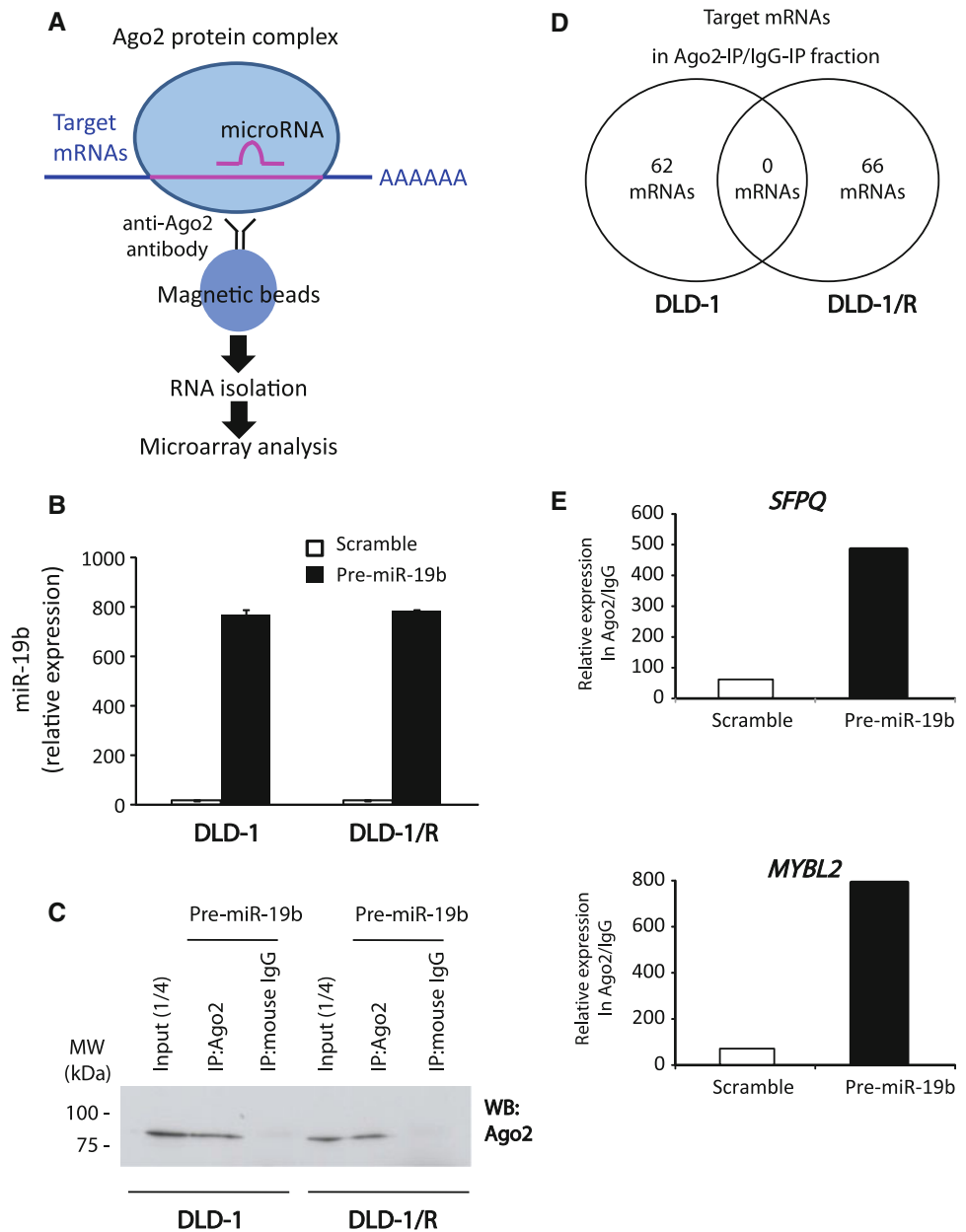
the Ago2-containing microRNA:mRNA complexes from DLD-1/R cells, as determined by qRT-PCR (Fig. 4e).

Discussion

Recent advances in microarray technologies have enabled us to measure global changes in microRNA expression using genome-wide surveys. Profiles of microRNA expression have been increasingly reported in various types of human malignancies, including colorectal cancer [34–36]. MicroRNA profiles are likely to be efficient as diagnostic tools to differentiate tumor types [16, 37], and have also been presented as biomarkers for tracing the tissue origins of cancers [17]. In addition, changes in microRNA expression have been proposed as determinants of pharmacologic responses [38]. Indeed, profiles of microRNA expression have been shown to be changed during treatment with anticancer drugs in several types of tumors [18, 19, 39–41]. These studies have offered an experimental base for the potential use of microRNAs in cancer therapy.

We found that the expression of miR-19b and miR-21 was related to the response to 5-FU treatment. Similarly, in a recent report [42], miR-19a (a paralogue of miR-19b) and miR-21 were up-regulated in HT29 and HCT-119 colon cancer cells in response to simple 5-FU exposure. These results support the idea that microRNA expression has a possible effect on drug resistance, at least 5-FU resistance.

Table 2 Top 15 target mRNAs of miR-19b enriched in anti-Ago2 complexes

Target genes	DLD-1		DLD-1/R		Genbank	Description
	Pre-miR-19b transfected	Control transfected	Pre-miR-19b transfected	Control transfected		
(A) DLD-1						
RGNEF	34.14	1.12	1.10>	1.63	AB082529	mRNA for KIAA1998 protein
PSG4	26.02	1.10>	1.30	1.10>	NM_213633	Pregnancy specific beta-1-glycoprotein 4 (PSG4), transcript variant 2
PIWIL4	24.12	1.10>	1.10>	1.10>	NM_152431	Piwi-like 4 (Drosophila) (PIWIL4)
USP34	23.44	1.10>	1.53	1.45	NM_014709	Ubiquitin specific peptidase 34 (USP34)
TTC9C	21.87	1.10>	1.10>	1.10>	NM_173810	Tetratricopeptide repeat domain 9C (TTC9C)
PRO2949	21.09	2.15	1.23	1.10>	AF119907	PRO2949 mRNA, complete cds
ALKBH6	18.22	1.10>	1.10>	1.10>	NM_198867	alkB, alkylation repair homolog 6 (E. coli) (ALKBH6), transcript variant 1
GCN5L2	17.90	1.10>	1.10>	1.10>	NM_021078	GCN5 general control of amino-acid synthesis 5-like 2 (yeast) (GCN5L2)
GRK4	14.26	1.10>	1.88	1.89	NM_001004057	G protein-coupled receptor kinase 4 (GRK4), transcript variant 3
DQ786237	11.44	1.10>	1.10>	1.10>	DQ786237	Clone HLS_IMAGE_1877990 mRNA sequence
ESRRB	11.43	1.10>	1.10>	1.10>	X51417	mRNA for steroid hormone receptor hERR2
RABGAP1L	10.58	1.10>	1.72	1.10>	AB007940	mRNA for KIAA0471 protein, partial cds
RNASE1	10.38	1.10>	1.10>	1.10>	S79281	Pancreatic ribonuclease [human, mRNA Recombinant Partial, 491 nt]
ST13	10.10	1.30	1.10>	1.10>	NM_003932	Suppression of tumorigenicity 13 (colon carcinoma) (Hsp70 interacting protein)
WDFY2	10.02	1.10>	1.10>	1.10>	NM_052950	WD repeat and FYVE domain containing 2 (WDFY2)
(B) DLD-1/R						
ABCA2	1.10>	1.10>	21.84	1.10>	NM_001606	ATP-binding cassette, sub-family A (ABC1), member 2 (ABCA2), transcript variant 1
BTN2A2	1.10	1.10>	21.64	1.10>	NM_181531	Butyrophilin, subfamily 2, member A2 (BTN2A2), transcript variant 2
LOC730589	1.10>	1.10>	20.74	1.38	XM_001126447	Hypothetical protein LOC730589
REM1	1.10>	1.10>	20.64	1.10>	NM_014012	RAS (RAD and GEM)-like GTP-binding 1 (REM1)
C1orf26	1.10>	1.10>	19.15	1.10>	NM_017673	Chromosome 1 open reading frame 26 (C1orf26)
SIRPB2	1.10>	1.10>	17.24	1.10>	AK095499	cDNA FLJ38180 fis, clone FCBBF1000121, weakly similar to Homo sapiens mRNA for SHPS-1
MED28	1.10>	1.10>	16.22	1.10>	NM_025205	Mediator of RNA polymerase II transcription, subunit 28 homolog (S. cerevisiae)
THC2531064	1.10>	1.10>	16.03	1.10>	THC2531064	Alu subfamily SQ sequence contamination warning entry, partial (11%)
TMEM107	1.10>	1.10>	14.77	1.10>	NM_032354	Transmembrane protein 107 (TMEM107), transcript variant 1
AF090938	1.10>	1.10>	14.34	1.10>	AF090938	Clone HQ0628 PRO0628 mRNA
CASQ1	1.10>	1.10>	14.18	1.10>	NM_001231	Calsequestrin 1 (fast-twitch, skeletal muscle), nuclear gene encoding mitochondrial protein
FLJ31659	2.52	1.10>	13.62	1.10>	NM_153027	Hypothetical protein FLJ31659
ZNF772	1.10>	1.43	13.22	1.10>	NM_001024596	Zinc finger protein 772 (ZNF772)
NDFIP1	1.10>	1.10>	12.05	1.10>	NM_030571	Nedd4 family interacting protein 1 (NDFIP1)
MYBL2	1.10>	1.10>	11.90	1.10>	NM_002466	v-myb myeloblastosis viral oncogene homolog (avian)-like 2 (MYBL2)

Fold enrichment mRNA (Ago2-IP/IgG-IP) was calculated. Boldface items indicate items computationally predicted with TargetScan

Table 3 Top 5 biofunctions of mRNAs enriched in anti-Ago2 complexes

Category	P value range	Molecules
(A) DLD-1		
Cell cycle	4.03E−04 to 4.31E−02	GRK4, **RBBP8**, IFNB1, RAC1, RPS6, **FGFR2**, SCMH1, KAT2A, PSEN1, ARID3A
Amino acid metabolism	1.22E−03 to 3.67E−02	ARL6IP5, PAX8, PSEN1
Cellular development	1.22E−03 to 4.86E−02	PPFIA1, IFNB1, RAC1, **FGFR2**, RPS6, BCCIP, MAP2K5, PSEN1
Molecular transport	1.22E−03 to 3.67E−02	ARL6IP5, PAX8, IFNB1, RAC1, PPP1CB, **FGFR2**, PSEN1
Small molecule biochemistry	1.22E−03 to 3.67E−02	ARL6IP5, PAX8, IFNB1, RAC1, **FGFR2**, PSEN1
(B) DLD-1/R		
Cell morphology	1.43E−03 to 3.78E−02	TRIO, REM1, GNAQ, MYBL2, ARHGEF11, SEMA6C
Cellular development	1.43E−03 to 4.28E−02	GNAQ, ARHGEF11, MED28, HDAC5
Cell cycle	2.57E−03 to 3.04E−02	SFPQ, MYBL2
Cell-to-cell signaling and interaction	2.57E−03 to 4.06E−02	TICAM1, GNAQ, MYBL2, OTUB2, HDAC5
Cellular assembly and organization	2.57E−03 to 4.77E−02	TRIO, REM1, CASQ1, GNAQ, ARHGEF11, STXBP5, HDAC5

Boldface items indicate items computationally predicted with TargetScan. Ingenuity pathway analysis (IPA) indicated the category of molecular and cellular functions with 62 mRNAs in DLD-1 cells and 66 mRNAs in DLD-1/R cells

However, only a limited number of microRNAs (<160) have been analyzed by qRT-PCR, and there have been no functional studies of the identified microRNAs [42]. Because of their imperfect base-pairing in target recognition, microRNAs can regulate several gene transcripts. With regard to predicting their possible target genes, there is a need for more direct experimental techniques to provide data about specific microRNA:mRNA interactions.

We found that the expression of miR-19b was up-regulated in DLD-1/R cells, in which there was no change in cell cycle profile after treatment with 5-FU. miR-19b is commonly derived from the miR-17-92 cluster, which encodes 6 mature microRNAs [43, 44]. This cluster is directly activated by a transcription factor that accumulates early in the G_1 phase of the cell cycle [43]. Although microRNAs generated from this cluster might have a function in the G_1 phase, it is largely unknown how they affect the cell cycle. We postulated that miR-19b might play an additional role in cell cycle progression and focused on its target mRNAs with RIP-Chip analysis. This approach has allowed us to identify potentially physiologically relevant targets of microRNAs and the complete target transcriptome [26, 32]. To our knowledge, this is the first report of RIP-Chip analysis of targets of miR-19b.

With the RIP-Chip method, a total of 128 gene transcripts were identified by >5.0-fold enrichment in the Ago2-IP fraction. However, our results do not provide complete confirmation of the prediction program. The prediction program for microRNA targets often predicts all possible targets irrespective of their physiological relevance [32]. Consequently, the false-positive rate can be high, and it is difficult to select the most relevant genes from a long list of predicted targets. The RIP-Chip

approach identified mRNAs which are associated with endogenous microRNAs in Ago2-containing complexes and thus enabled us to conduct direct screening of any human cell type.

We applied IPA software to uncover the possible functional pathways used by target genes associated with miR-19b. IPA is a tool for comparing novel data sets to an existing library of knowledge-based cellular and molecular pathways [27]. Interestingly, IPA ranked "Cell Cycle" in the top 5 of biofunctions modified by 128 target genes in miR-19b over-expressed cells (Table 3). Of note, up-regulation of miR-19b expression was observed in DLD-1/R cells in response to 5-FU, from which *SFPQ* (splicing factor proline and glutamate-rich) and *MYBL2* (v-Myb myeloblastosis viral oncogene homolog-like2) were detected in microRNA:mRNA complexes as targets of miR-19b. This supports a significant role for these target genes in the regulation of the cell cycle. *SFPQ* potentially plays an important role during different stages of mRNA processing as part of the spliceosome complex and transport [45]. *SFPQ* has functions at different cell cycle stages to maintain sister chromatid interaction [46], and depletion of this gene has been found to cause abnormal accumulation of cells in the S phase of the cell cycle [47]. *MYBL2* (also known as *b-Myb*) is a member of a family of transcription factors involved in the control of cell cycle progression [48]. *MYBL2* is directly regulated by E2F transcription factors and is maximally induced at the G1/S boundary of the cell cycle [49]. However, little is known about the functional control of these genes by microRNAs. Through the control of microRNAs, *SFPQ* and *MYBL2* may contribute to the uncharacterized mechanisms of cell cycle responses to treatment by 5-FU.

In conclusion, we have identified up-regulation of miR-19b in 5-FU-resistant colon cancer cells, which show no alteration in their cell cycles in response to the drug. To identify the specific microRNA:mRNA interactions, RIP-Chip analysis was used to find previously uncharacterized targets of miR-19b. Using knowledge-based pathway analysis, a possible connection was found between target mRNAs associated with miR-19b and the cell cycle. For exploring the unidentified mechanisms of drug resistance, this is an important improvement over previous methods as an unbiased identification of relevant target genes of microRNAs.

References

1. Jemal A, Siegel R, Xu J, et al. Cancer statistics, 2010. CA Cancer J Clin. 2010;60:277–300.
2. Efficacy of adjuvant fluorouracil and folinic acid in colon cancer. International Multicentre Pooled Analysis of Colon Cancer Trials (IMPACT) investigators. Lancet. 1995; 345:939–44.
3. Douillard JY, Cunningham D, Roth AD, et al. Irinotecan combined with fluorouracil compared with fluorouracil alone as first-line treatment for metastatic colorectal cancer: a multicentre randomised trial. Lancet. 2000;355:1041–7.
4. Dean M, Fojo T, Bates S. Tumour stem cells and drug resistance. Nat Rev Cancer. 2005;5:275–84.
5. Iorns E, Lord CJ, Turner N, et al. Utilizing RNA interference to enhance cancer drug discovery. Nat Rev Drug Discov. 2007;6:556–68.
6. Mariadason JM, Arango D, Shi Q, et al. Gene expression profiling-based prediction of response of colon carcinoma cells to 5-fluorouracil and camptothecin. Cancer Res. 2003;63:8791–812.
7. Boyer J, Allen WL, McLean EG, et al. Pharmacogenomic identification of novel determinants of response to chemotherapy in colon cancer. Cancer Res. 2006;66:2765–77.
8. Ooyama A, Takechi T, Toda E, et al. Gene expression analysis using human cancer xenografts to identify novel predictive marker genes for the efficacy of 5-fluorouracil-based drugs. Cancer Sci. 2006;97:510–22.
9. Karasawa H, Miura K, Fujibuchi W, et al. Down-regulation of cIAP2 enhances 5-FU sensitivity through the apoptotic pathway in human colon cancer cells. Cancer Sci. 2009;100:903–13.
10. Bartel DP. MicroRNAs: genomics, biogenesis, mechanism, and function. Cell. 2004;116:281–97.
11. He L, Hannon GJ. MicroRNAs: small RNAs with a big role in gene regulation. Nat Rev Genet. 2004;5:522–31.
12. Nilsen TW. Mechanisms of microRNA-mediated gene regulation in animal cells. Trends Genet. 2007;23:243–9.
13. Pillai RS, Bhattacharyya SN, Filipowicz W. Repression of protein synthesis by miRNAs: how many mechanisms? Trends Cell Biol. 2007;17:118–26.
14. Miranda KC, Huynh T, Tay Y, et al. A pattern-based method for the identification of MicroRNA binding sites and their corresponding heteroduplexes. Cell. 2006;126:1203–17.
15. Kloosterman WP, Plasterk RH. The diverse functions of microRNAs in animal development and disease. Dev Cell. 2006;11:441–50.
16. Rosenfeld N, Aharonov R, Meiri E, et al. MicroRNAs accurately identify cancer tissue origin. Nat Biotechnol. 2008;26:462–9.
17. Calin GA, Croce CM. MicroRNA signatures in human cancers. Nat Rev Cancer. 2006;6:857–66.
18. Si ML, Zhu S, Wu H, et al. miR-21-mediated tumor growth. Oncogene. 2007;26:2799–803.
19. Yang H, Kong W, He L, et al. MicroRNA expression profiling in human ovarian cancer: miR-214 induces cell survival and cisplatin resistance by targeting PTEN. Cancer Res. 2008;68:425–33.
20. Murakami Y, Kazuno H, Emura T, et al. Different mechanisms of acquired resistance to fluorinated pyrimidines in human colorectal cancer cells. Int J Oncol. 2000;17:277–83.
21. Fukushima M, Fujioka A, Uchida J, et al. Thymidylate synthase (TS) and ribonucleotide reductase (RNR) may be involved in acquired resistance to 5-fluorouracil (5-FU) in human cancer xenografts in vivo. Eur J Cancer. 2001;37:1681–7.
22. Boyer J, McLean EG, Aroori S, et al. Characterization of p53 wild-type and null isogenic colorectal cancer cell lines resistant to 5-fluorouracil, oxaliplatin, and irinotecan. Clin Cancer Res. 2004;10:2158–67.
23. Schroeder A, Mueller O, Stocker S, et al. The RIN: an RNA integrity number for assigning integrity values to RNA measurements. BMC Mol Biol. 2006;7:3.
24. Allison DB, Cui X, Page GP, et al. Microarray data analysis: from disarray to consolidation and consensus. Nat Rev Genet. 2006;7:55–65.
25. Zhang X, Chen J, Radcliffe T, et al. An array-based analysis of microRNA expression comparing matched frozen and formalin-fixed paraffin-embedded human tissue samples. J Mol Diagn. 2008;10:513–9.
26. Wang WX, Wilfred BR, Hu Y, et al. Anti-Argonaute RIP-Chip shows that miRNA transfections alter global patterns of mRNA recruitment to microribonucleoprotein complexes. RNA. 2010;16:394–404.
27. Calvano SE, Xiao W, Richards DR, et al. A network-based analysis of systemic inflammation in humans. Nature. 2005;437:1032–7.
28. Mu P, Han YC, Betel D, et al. Genetic dissection of the miR-17 ∼ 92 cluster of microRNAs in Myc-induced B-cell lymphomas. Genes Dev. 2009;23:2806–11.
29. Olive V, Bennett MJ, Walker JC, et al. miR-19 is a key oncogenic component of mir-17-92. Genes Dev. 2009;23:2839–49.
30. Giovannetti E, Funel N, Peters GJ, et al. MicroRNA-21 in pancreatic cancer: correlation with clinical outcome and pharmacologic aspects underlying its role in the modulation of gemcitabine activity. Cancer Res. 2010;70:4528–38.
31. Wang H, Ach RA, Curry B. Direct and sensitive miRNA profiling from low-input total RNA. RNA. 2007;13:151–9.
32. Tan LP, Seinen E, Duns G, et al. A high throughput experimental approach to identify miRNA targets in human cells. Nucleic Acids Res. 2009;37:e137.
33. Hayashida Y, Nishibu T, Inoue K, et al. A useful approach to total analysis of RISC-associated RNA. BMC Res Notes. 2009;2:169.
34. Schetter AJ, Leung SY, Sohn JJ, et al. MicroRNA expression profiles associated with prognosis and therapeutic outcome in colon adenocarcinoma. JAMA. 2008;299:425–36.
35. Schepeler T, Reinert JT, Ostenfeld MS, et al. Diagnostic and prognostic microRNAs in stage II colon cancer. Cancer Res. 2008;68:6416–24.

36. Lanza G, Ferracin M, Gafa R, et al. mRNA/microRNA gene expression profile in microsatellite unstable colorectal cancer. Mol Cancer. 2007;6:54.

37. Murakami Y, Yasuda T, Saigo K, et al. Comprehensive analysis of microRNA expression patterns in hepatocellular carcinoma and non-tumorous tissues. Oncogene. 2006;25:2537–45.

38. Blower PE, Chung JH, Verducci JS, et al. MicroRNAs modulate the chemosensitivity of tumor cells. Mol Cancer Ther. 2008;7:1–9.

39. Meng F, Henson R, Lang M, et al. Involvement of human micro-RNA in growth and response to chemotherapy in human cholangiocarcinoma cell lines. Gastroenterology. 2006;130:2113–29.

40. Kovalchuk O, Filkowski J, Meservy J, et al. Involvement of microRNA-451 in resistance of the MCF-7 breast cancer cells to chemotherapeutic drug doxorubicin. Mol Cancer Ther. 2008;7:2152–9.

41. Xia L, Zhang D, Du R, et al. miR-15b and miR-16 modulate multidrug resistance by targeting BCL2 in human gastric cancer cells. Int J Cancer. 2008;123:372–9.

42. Rossi L, Bonmassar E, Faraoni I. Modification of miR gene expression pattern in human colon cancer cells following exposure to 5-fluorouracil in vitro. Pharmacol Res. 2007;56:248–53.

43. O'Donnell KA, Wentzel EA, Zeller KI, et al. c-Myc-regulated microRNAs modulate E2F1 expression. Nature. 2005;435:839–43.

44. Mendell JT. miRiad roles for the miR-17-92 cluster in development and disease. Cell. 2008;133:217–22.

45. Gozani O, Patton JG, Reed R. A novel set of spliceosome-associated proteins and the essential splicing factor PSF bind stably to pre-mRNA prior to catalytic step II of the splicing reaction. EMBO J. 1994;13:3356–67.

46. Rajesh C, Baker DK, Pierce AJ, et al. The splicing-factor related protein SFPQ/PSF interacts with RAD51D and is necessary for homology-directed repair and sister chromatid cohesion. Nucleic Acids Res. 2011;39:132–45.

47. Salton M, Lerenthal Y, Wang SY, et al. Involvement of Matrin 3 and SFPQ/NONO in the DNA damage response. Cell Cycle. 2010;9:1568–76.

48. Oh IH, Reddy EP. The myb gene family in cell growth, differentiation and apoptosis. Oncogene. 1999;18:3017–33.

49. Joaquin M, Watson RJ. Cell cycle regulation by the B-Myb transcription factor. Cell Mol Life Sci. 2003;60:2389–401.